

Electronic Supporting Information

Isolated PdO sites on SiO₂-supported NiO nanoparticles as active sites for allylic alcohol selective oxidation

Aleksandra Ziarko,^a Thomas J. A. Slater,^b Mark A. Isaacs,^{c,d} Lee J. Durndell,^e and Christopher M. A. Parlett^{f,g,h,i,*}

- Department of Chemical Engineering and Applied Chemistry, Aston University, Birmingham, B4 7ET, UK.
- School of Chemistry, Cardiff University, Cardiff, CF10 3AT, UK.
- Department of Chemistry, University College London, London, WC1H 0AJ, UK.
- HarwellXPS, Research Complex at Harwell, RAL, Harwell Campus, Didcot, OX11 0FA, UK.
- School of Geography, Earth and Environmental Sciences, University of Plymouth, Plymouth, PL4 8AA, UK.
- Department of Chemical Engineering, University of Manchester, Manchester, M13 9PL, UK.
- University of Manchester at Harwell, Diamond Light Source, Rutherford Appleton Laboratory, Didcot, Oxfordshire, OX11 0DE, UK.
- Diamond Light Source, Rutherford Appleton Laboratory, Didcot, Oxfordshire, OX11 0DE, UK.
- UK Catalysis Hub, Research Complex at Harwell, Rutherford Appleton Laboratory, Oxfordshire, OX11 0FA, UK.

Email: christopher.parlett@manchester.ac.uk

Methodology

Mesoporous Silica Nanospheres (SiO₂): Cetyltrimethylammonium chloride (240 cm³, 25% w/w in water) and triethanolamine (1.8 g) were added to deionised water (360 cm³) and stirred at 400 RPM 60°C for 0.5 hours in a 1 L round-bottom flask. Agitation was reduced to 150 RPM and Tetraethylorthosilicate (40 cm³) in cyclohexane 160 (cm³) was carefully laid on top of the aqueous phase to form a biphasic reaction media. The reaction was agitated at 150 RPM 60°C for 48 hours. The organic phase was removed, and the as-synthesised solid silica was recovered from the aqueous phase by centrifuging at 14500 RPM for 15 minutes and washed 3 times with water (500 cm³). The solid was dried at 100°C for 24 hours before calcination in air at 600 °C (ramp rate 1 °C min⁻¹).

Ethylene glycol assisted Ni impregnation (NiO/SiO₂): SiO₂ (1.5 g) was stirred in an aqueous impregnation solution (8 ml) containing nickel nitrate hexahydrate to give a nominal metal loading of 5 wt.% and ethylene glycol (1:1 Ni:glycol mol ratio) for 16 h. The solution was heated to 50 °C and stirred for 8 h to form a dry powder. The resulting solid was calcined at 400 °C for 2 h in air (ramp rate 1 °C min⁻¹).

Galvanic Pd deposition onto NiO (NiO@PdO/SiO₂): NiO/SiO₂ (1 g) was stirred at 500 rpm in an aqueous ammonium tetrachloropalladate(II) solution (1mM, 100 cm³) for 6 hours at room temperature. The solid was isolated by centrifuging at 14500 RPM for 15 minutes and washed 3 times with water (100 cm³). The solid was dried at 100 °C for 16 hours.

Catalyst reduction (NiO@PdO/SiO₂red): The impact of catalyst reduction on catalytic performance was evaluated by thermal reduction of NiO@PdO/SiO₂ at 600 °C for 1 hour under flowing H₂ (ramp rate 5 °C min⁻¹, H₂ flow rate 10 ml min⁻¹).

Characterisation: Nitrogen porosimetry was undertaken on a Quantachrome Quadrasorb porosimeter. Samples were degassed at 150 °C for 6 h before recording N₂ adsorption/desorption isotherms. BET (Brunauer, Emmett and Teller) surface areas were calculated over the relative pressure range 0.02–0.2. Mesopore properties were calculated by applying the BJH (Barrett–Joyner–Halenda) method to the desorption isotherm for relative pressures >0.35. Powder X-ray diffraction patterns (XRD) were recorded using a benchtop Rigaku Miniflex 600, with a 600 W Cu X-ray tube source and a

D-tex Ultra-high-speed silicon strip detector. Samples were measured from 2θ of 30° to 80° with a step of 0.02° and a speed of 2° per minute. High-resolution (scanning) transmission electron microscopy (S)TEM images were recorded on either a JEOL 2100F FEG STEM operating at 200 keV and equipped with a spherical aberration probe corrector (CEOS GmbH) and a Bruker XFlash 5030 EDX or on a double aberration-corrected JEOL ARM300CF operating at 300 keV with a Cs corrector and Oxford Instruments XMAX 100 EDX detector At Diamond Light Source (Beamline I14 EPSIC). Samples were prepared for microscopy by dispersing in methanol and drop-casting onto a copper grid coated with a holey carbon support film (Agar Scientific). Images were analysed using ImageJ 1.41 software. Elemental analysis was conducted by X-ray fluorescence (XRF) on a Horiba XGT-7000 X-ray analytical microscope fitted with a rhodium X-ray tube, operating at 50 kV, with a spot size of 1.2 mm, and a silicon detector. Samples were analysed under vacuum, with quantification using the K emission line of each element and assuming all to be present as their oxide. At least 20 Spectra from different spatial locations within the powder sample were collected with an acquisition time of 10 seconds per spectra. Galvanic displacement solutions were analysed by microwave plasma atomic emission spectrometry on an Agilent 4200 MP-AES, with the instrument calibrated using Pd and Ni standard solutions. Temperature programmed reduction (TPR) was conducted on a Quantachrome ChemBET PULSAR TPR/TPD. Samples were analysed under flow H₂ (10% H₂ in N₂ at a flow rate of 20 cm³ min⁻¹) up to 800 °C (ramp rate 10 °C min⁻¹). Transmission Pd K-edge and Ni K-edge X-ray absorption spectroscopy (XAS) was conducted on beamline B18 at Diamond Light source. Samples were prepared as pressed pellets diluted with BN, where required, to give an edge jump of ~ 1 . Reference standards were also collected. Data analysis was conducted using IFEFFIT version 1.2.12 open-source software, with Athena version 0.9.26 for normalisation, background subtraction and linear combination fitting of XANES, and Artemis version 0.9.26 for EXAFS fitting.

Cinnamyl alcohol selox: Catalyst screening was performed at 50 cm³ scale at 80 °C under oxygen (10 cm³ min⁻¹ at 1 bar) bubbled through the solution via 0.5 mm internal diameter PTFE tubing with agitation at 1000 rpm. 100 mg of NiO@PdO/SiO₂ catalyst was added to the reaction media containing cinnamyl alcohol (4.43 g, 33 mmol) and mesitylene (0.5 cm³), as an internal standard, in toluene (50 cm³). Aliquots (0.25 cm³) were taken periodically, filtered, and diluted with toluene (1.75 cm³) for reaction monitoring via GC analysis. Initial rates and TOFs (based on XAS PdO content) were calculated at low conversion (< 10%) from the initial linear region of the alcohol conversion profiles (typically 10-15 minutes), with selectivity and mass balances (mass balanced were > 98% for the initial period and > 94% after 6 hours) calculated using calibrated response factors for reactants and products. The catalyst was recovered at the end of the reaction by filtration, with recycle studies conducted at an appropriately adjusted scale.

XAS Operando Cinnamyl alcohol selox: Fluorescence Pd K-edge XAS were collected at Diamond Light Source on beamline B18 employing a Si [3 1 1] monochromator, Pt-coated mirrors, and a Vortex multichannel fluorescence detector. Operando XAS spectra were continuously acquired over 6 hours with spectra acquisition of ~ 3 minutes, using Kapton tubing as an operando recirculating cell. A reaction slurry of 100 mg catalyst and cinnamyl alcohol (4.4276 g, 33 mmol), toluene (50 cm³) mesitylene (0.5 cm³) was continuously recirculated through the cell from the heated reaction reservoir at 80 °C under bubbling O₂ (1 bar pressure at 10 cm³ min⁻¹) with stirring at 1000 rpm.

Results

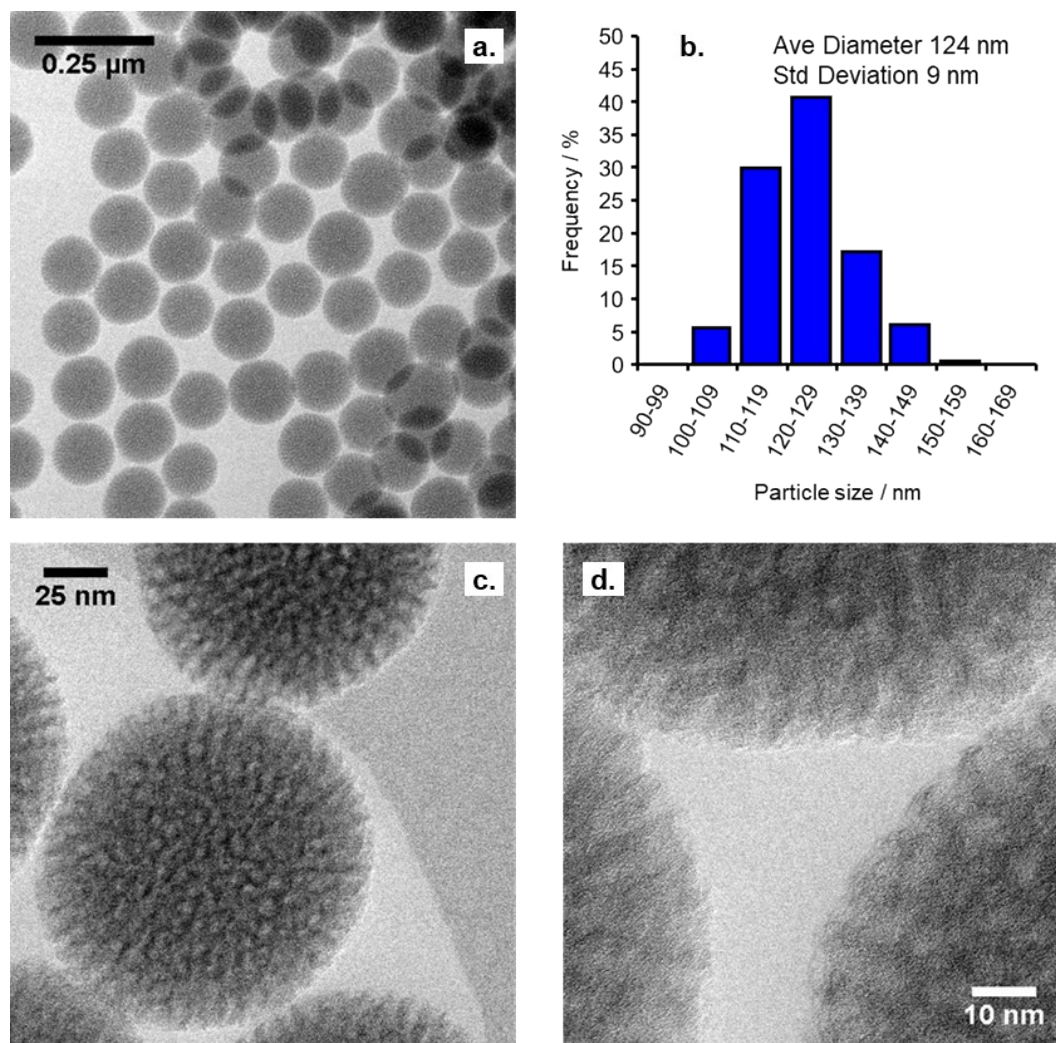


Figure S1. a., c., and d. BF-STEM of SiO₂ nanospheres, with b. nanosphere particle size distribution.

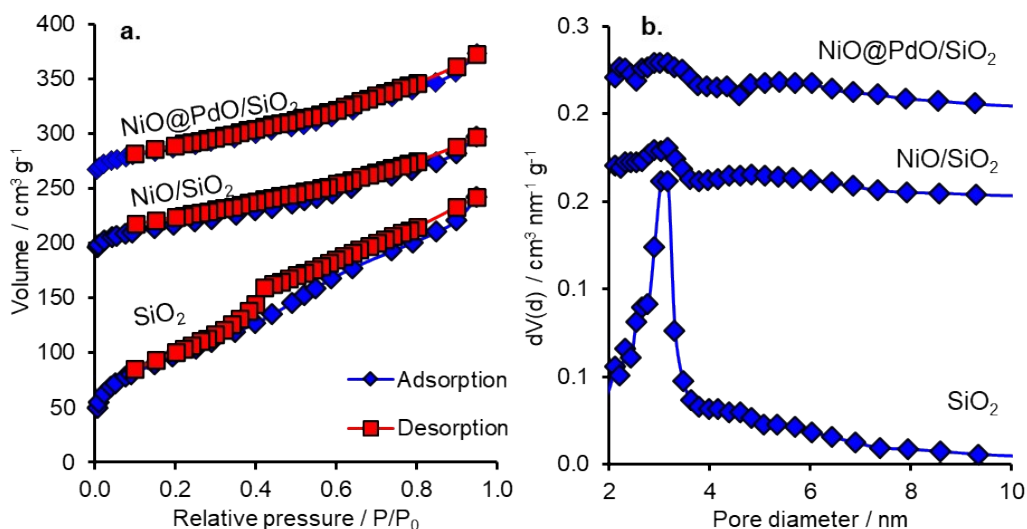


Figure S2. **a.** Stacked N₂ adsorption isotherms of SiO₂, NiO/SiO₂ (offset by 175) and NiO@PdO/SiO₂ (offset by 225), **b.** stacked BJH plots from desorption branch of the N₂ isotherm of SiO₂, NiO/SiO₂ (offset by 1.15) and NiO@PdO/SiO₂ (offset by 0.2).

Table S1. Physical properties of SiO₂, NiO/SiO₂ and NiO@PdO/SiO₂.

Sample	BET / m ² g ⁻¹ ^a	Pore Vol/ cm ³ g ⁻¹ ^a	BJH / nm ^b	NiO particle size / nm ^c
SiO ₂	348	0.99	3.2	n/a
NiO/SiO ₂	150	0.65	3.1	2.2 (±0.5)
NiO@PdO/SiO ₂	134	0.66	3	2.6 (±0.5)

a – N₂ adsorption isotherms, b – BJH from N₂ desorption branch, c- Scherer analysis of NiO(220) peak from XRD patterns

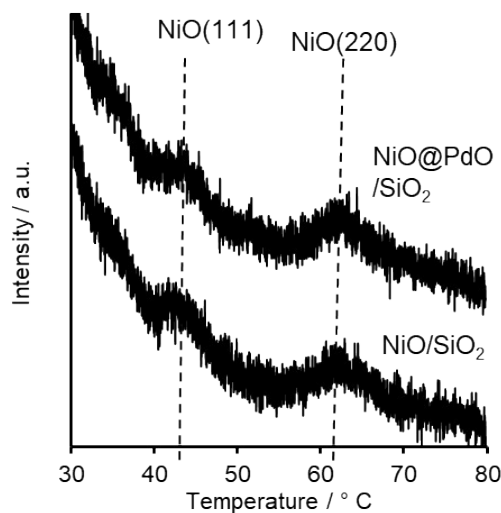


Figure S3. Stacked XRD patterns for NiO/SiO₂ and NiO@PdO/SiO₂ (offset for visualisation).

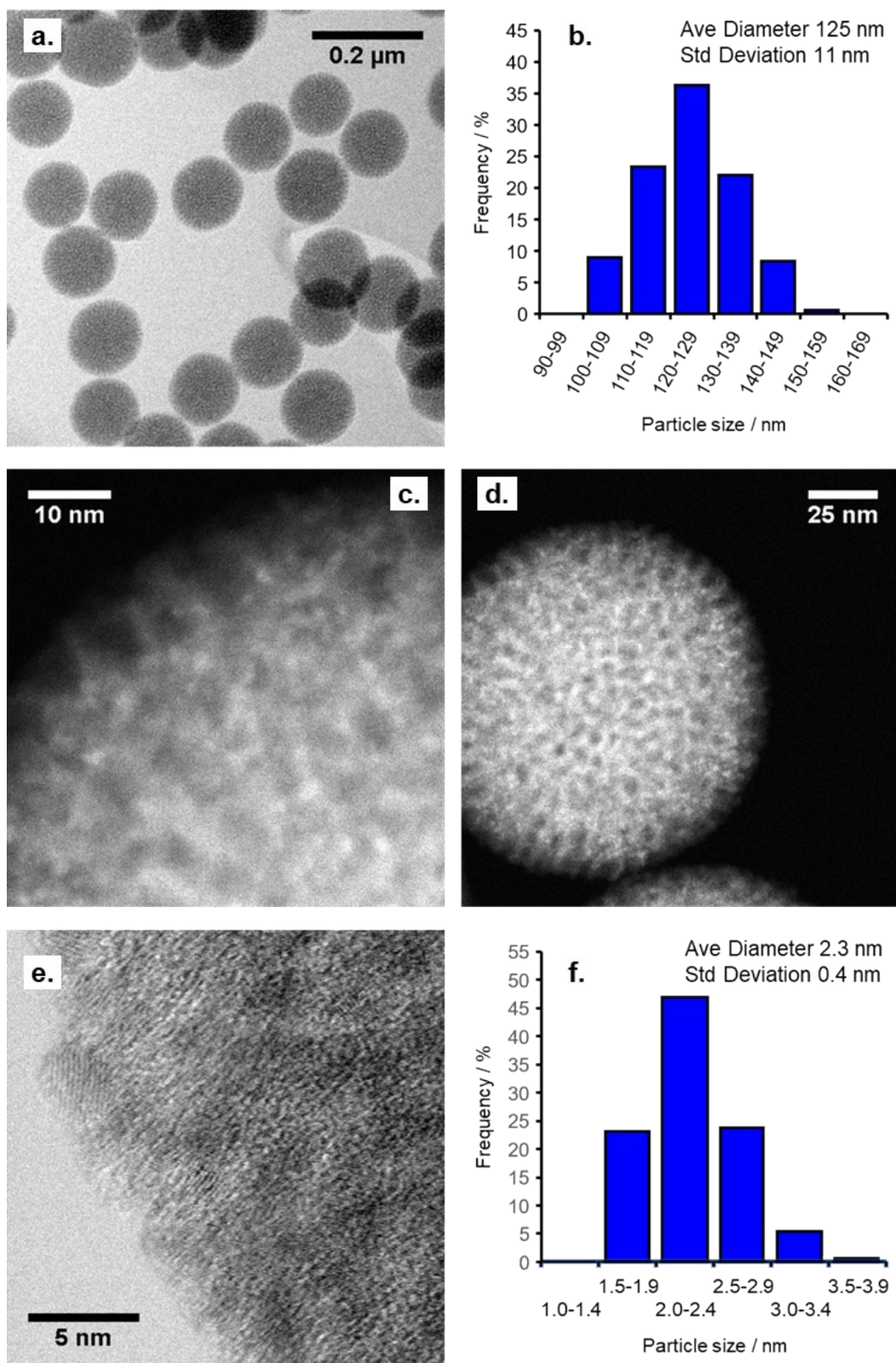


Figure S4. **a.** BF-STEM of NiO/SiO₂ nanospheres, **b.** NiO/SiO₂ nanosphere particle size distribution, **c.** and **d.** HAADF-STEM of NiO/SiO₂, **e.** BF-STEM of NiO/SiO₂, and **f.** NiO nanoparticle size distribution.

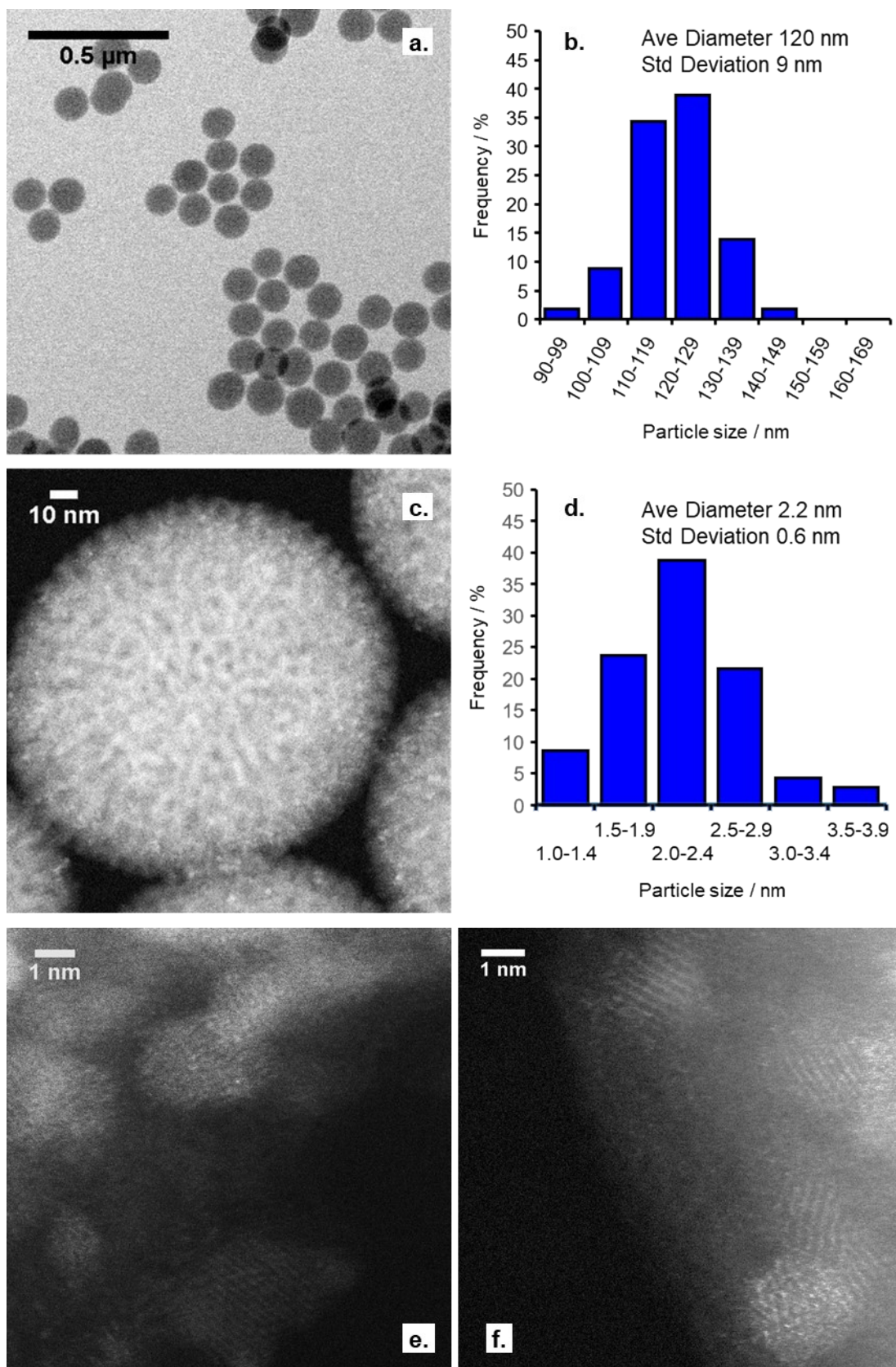


Figure S5. **a.** BF-STEM of $\text{NiO}@PdO/\text{SiO}_2$ nanospheres, **b.** $\text{NiO}@PdO/\text{SiO}_2$ nanosphere particle size distribution, **c.** HAADF-STEM of $\text{NiO}@PdO/\text{SiO}_2$, **d.** $\text{NiO}@PdO$ nanoparticle size distribution, and **e.** and **f.** showing HAADF-STEM of individual $\text{NiO}@PdO/\text{SiO}_2$ particles identifying isolate Pd sites on NiO.

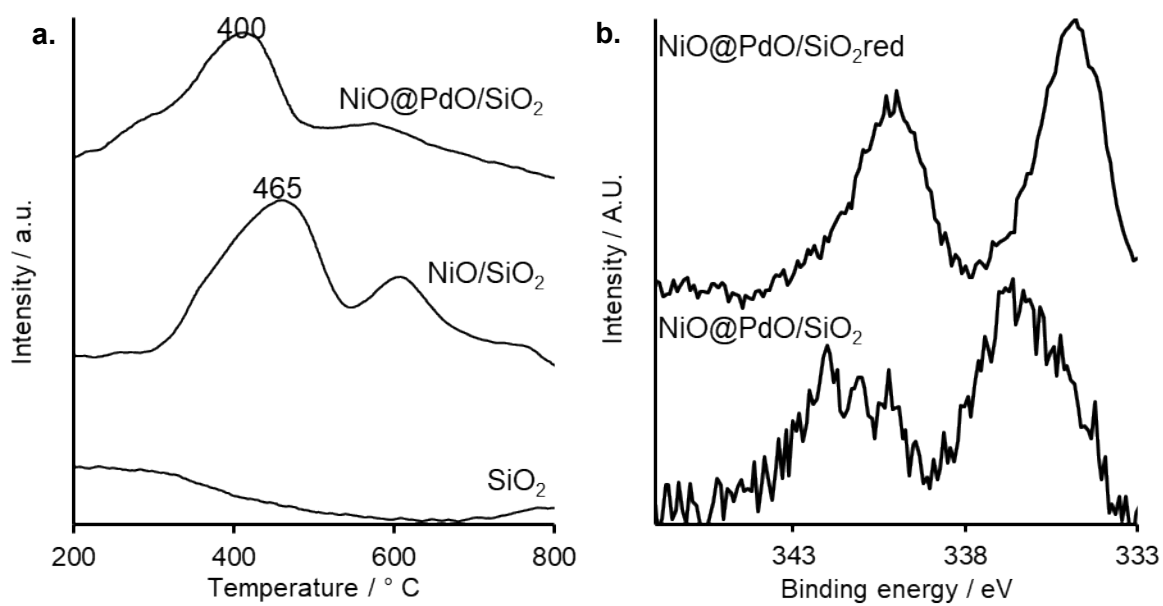


Figure S6. a. Stacked TPR of SiO₂, NiO/SiO₂ and NiO@PdO/SiO₂ (offset for visualisation), b. Stacked ex-situ Pd 3d XPS for NiO@PdO/SiO₂ and NiO@PdO/SiO₂red (offset for visualisation).

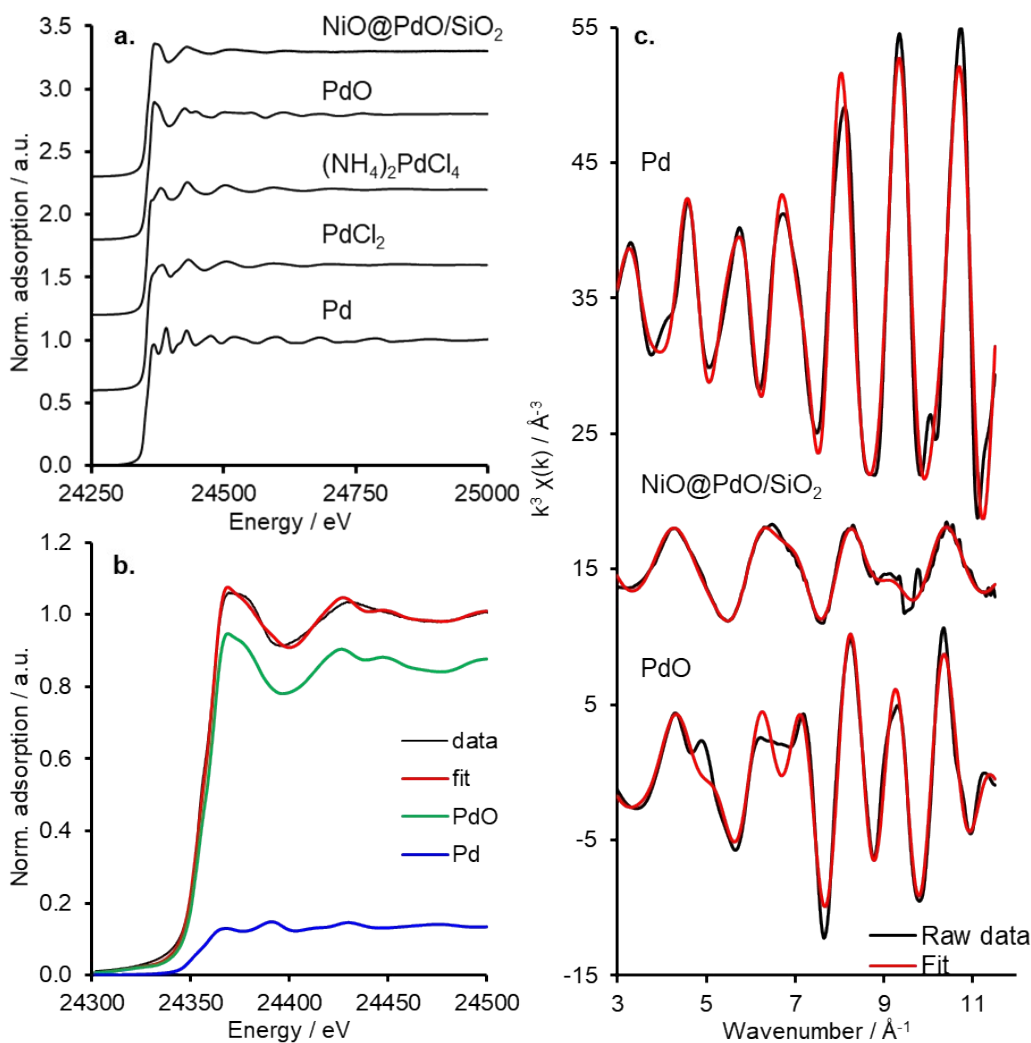


Figure S7. **a.** Stacked ex-situ Pd K edge XAS of NiO@PdO/SiO₂ and Pd standards (offset for visualisation), **b.** XANES linear combination fitting of NiO@PdO/SiO₂, and **c.** stacked ex-situ k³-weighted EXAFS data and fits for NiO@PdO/SiO₂, PdO, and Pd standards.

Table S2. Pd K edge EXAFS fitting parameters for NiO@PdO/SiO₂, PdO, and Pd standards.

Sample	Path	CN	R / Å	σ^2	R-factor
PdO	Pd-O	4	2.0295	0.00271	0.062
	Pd-Pd(II)	4	3.0483	0.00514	
	Pd-Pd(II)	8	3.4391	0.00616	
PdO@NiO/SiO ₂	Pd-O	3.9	2.0365	0.00451	0.029
	Pd-Pd(II)/Ni(II)	1.7	3.0589	0.00883	
Ex-situ	Pd-Pd(II)/Ni(II)	3.5	3.4511	0.01517	0.025
	Pd-Pd(0)	12	2.7444	0.00585	
	Pd-Pd(0)	6	3.8812	0.0055	
Pd	Pd-Pd(0)	24	4.7525	0.0096	

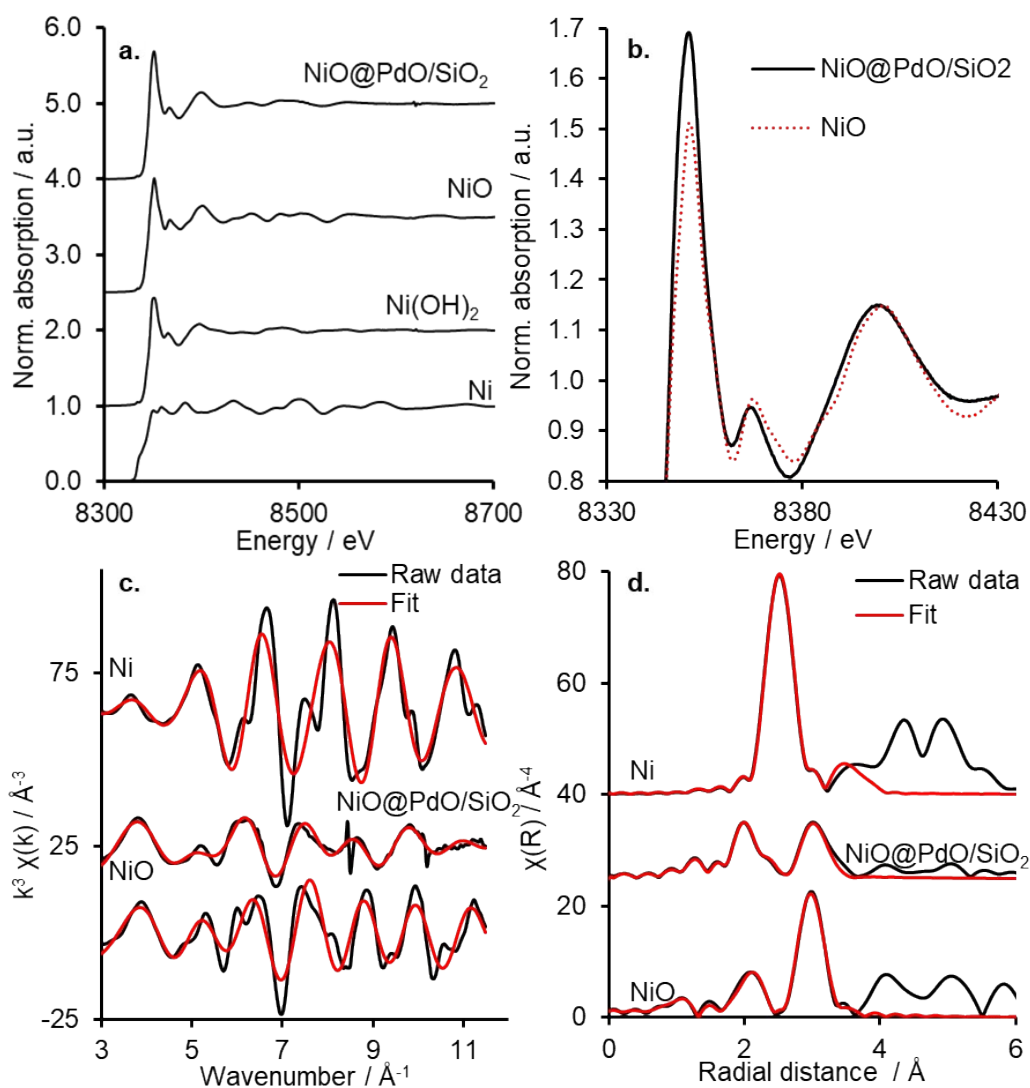


Figure S8. **a.** Stacked ex-situ Ni K-edge XAS of NiO@PdO/SiO₂ and Ni standards (offset for visualisation), **b.** Increased white line intensity of NiO@PdO/SiO₂ compared to NiO, n fitting of NiO@PdO/SiO₂, **c.** stacked ex-situ k₃-weighted EXAFS data and fits for NiO@PdO/SiO₂, PdO, and Pd standards, and **d.** stacked corresponding EXAFS Fourier transforms.

Table S3. Ni K edge EXAFS fitting parameters for NiO@PdO/SiO₂, NiO, and Ni standards.

Sample	Path	CN	R / Å	σ^2	R-factor
NiO	Ni-O	6	2.09068	0.00691	0.1255
	Ni-Ni(II)	12	2.95666	0.00675	
PdO@NiO/SiO ₂ ex-situ	Ni-O	1.0	1.9964	0.00151	0.0918
	Ni-O	6.1	2.0879	0.00867	
	Ni-Ni(II)	9.2	3.0019	0.01057	
Ni	Ni-Ni	12	2.4846	0.00615	0.1287
	Ni-Ni	6	3.5137	0.00897	

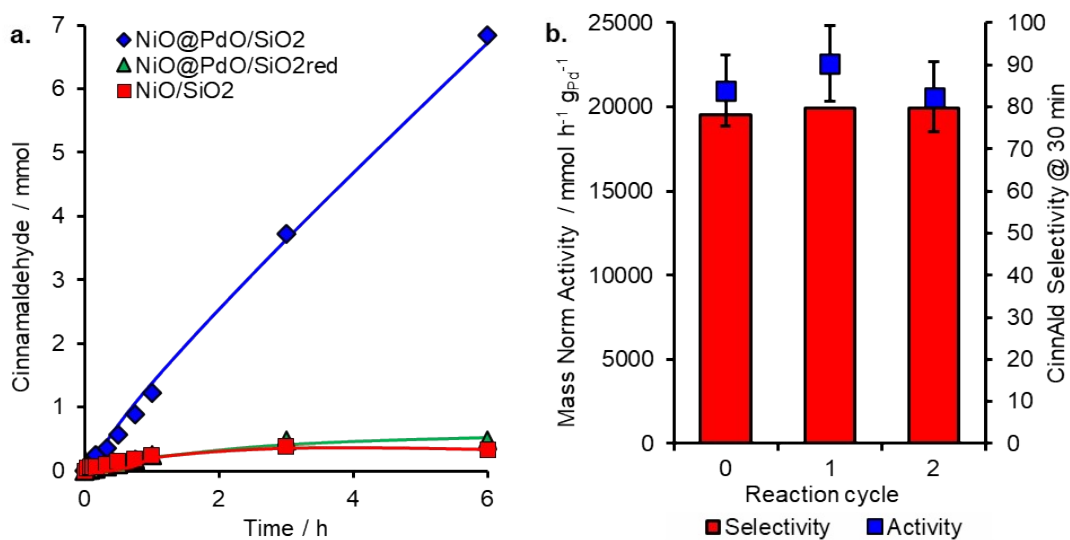


Figure S9. a. Cinnamaldehyde production over NiO@PdO/SiO₂, NiO@PdO/SiO₂red and NiO/SiO₂. b. Initial cinnamyl alcohol selox performance, prior to apparent deactivation from reaction kinetics, for NiO@PdO/SiO₂ as prepared and 2 subsequent recycles.

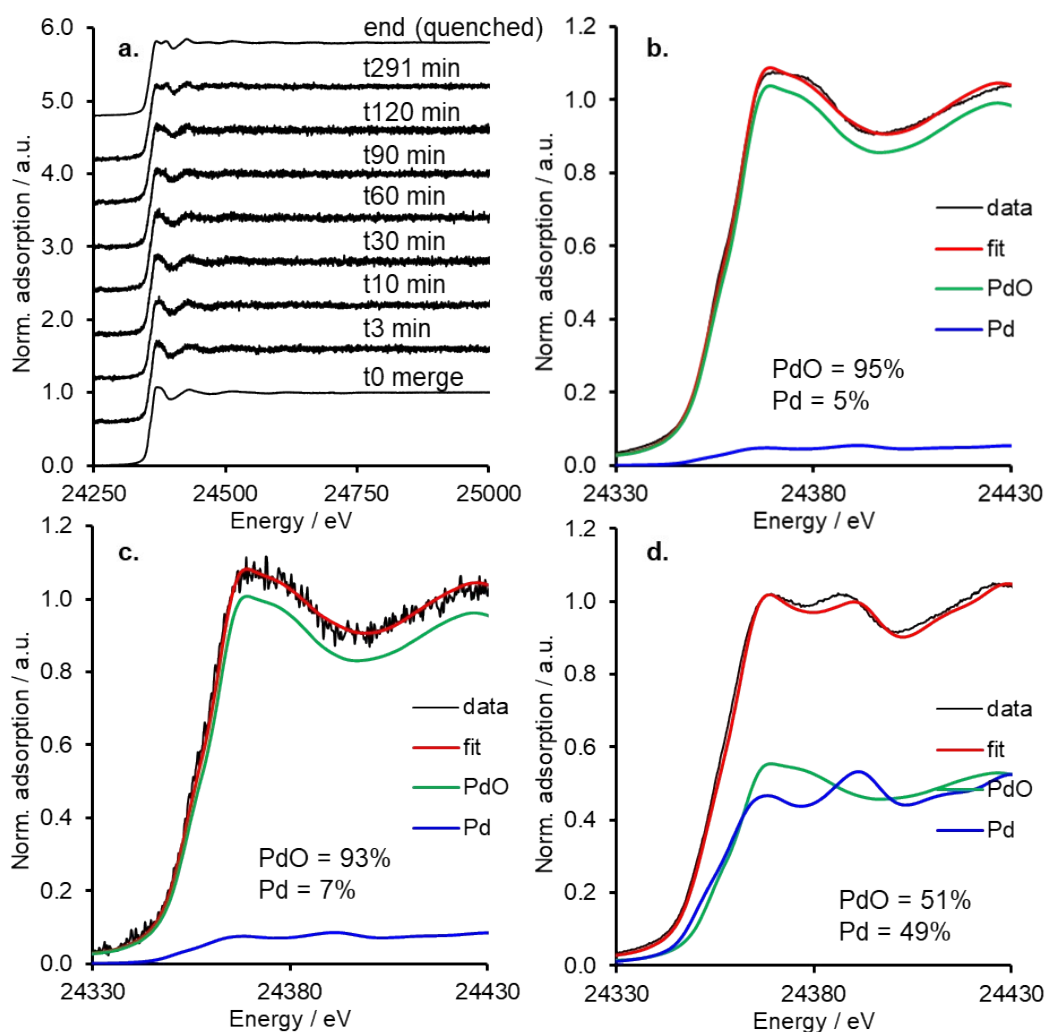


Figure S10. a. Stacked Pd K-edge operando XAS during cinnamyl alcohol selox over NiO@PdO/SiO₂ (only selected time points show and stacked for visualisation), b. XANES LCF at t₀, c. XANES LCF at 5 minutes, and d. XANES LCF at 6 hours (end).

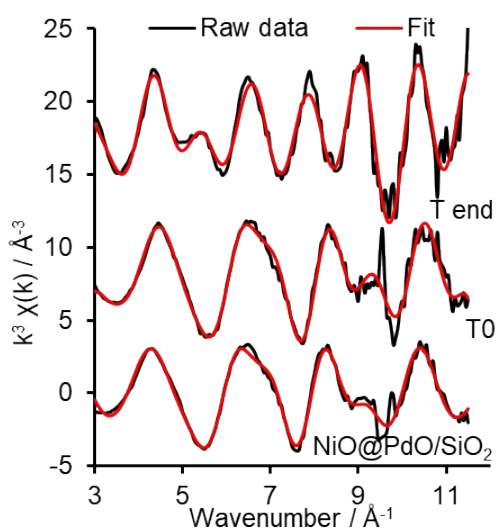


Figure S11. Stacked Pd K-edge operando k₃-weighted EXAFS data and fits for NiO@PdO/SiO₂ at t₀ and 6 hours (end), compared to the sample measured ex-situ.

Table S4. Pd K edge operando EXAFS fitting parameters for NiO@PdO/SiO₂ at t₀ and 6 hours, compared to the sample measured ex-situ.

Sample	Path	CN	R / Å	σ^2	R-factor
PdO@NiO/SiO ₂ ex-situ	Pd-O	3.9	2.0365	0.00451	0.029
	Pd-Pd(II)/Ni(II)	1.7	3.0589	0.00883	
	Pd-Pd(II)/Ni(II)	3.5	3.4511	0.01517	
PdO@NiO/SiO ₂ T0	Pd-O	4.5	2.0379	0.00339	0.042
	Pd-Pd(II)/Ni(II)	1.1	3.0611	0.00561	
	Pd-Pd(II)/Ni(II)	2.9	3.4535	0.01426	
PdO@NiO/SiO ₂ T6 hours (end) i.e. quenched to room temp.	Pd-O	2.5	2.0236	0.0068	0.059
	Pd-Pd(0)/Ni(0)	4.2	2.8069	0.00651	
	Pd-Pd(II)/Ni(II)	2.5	3.0395	0.02182	
	Pd-Pd(II)/Ni(II)	5.0	3.4292	0.02227	